Chemical Engineering & Processing: Process Intensification 222 (2026) 110750

Contents lists available at ScienceDirect

Chemical Engineering and Processing - Process Intensification

journal homepage: www.elsevier.com/locate/cep

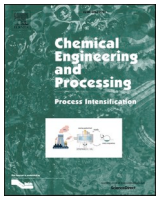

Magnetic actuation of fungal pellets via immobilization of ferromagnetic particles

Lukas Hartmann [a], Marina Schreidl [a], Markus Pyschik [b], Markus Stöckl [b], Dirk Holtmann [a,*]

[a] Karlsruhe Institute of Technology, Kaiserstr. 12, 76131 Karlsruhe, Germany
[b] DECHEMA Research Institute, Theodor-Heuss-Allee 25, 60486 Frankfurt am Main, Germany

ARTICLE INFO

Keywords:
Intensification of fungal cultivation
Microparticle-enhanced cultivation
Magnetic particle
Magnetic biomass
Immobilization
Aspergillus oryzae

ABSTRACT

Magnetic functionalization of fungal biomass via *in situ* immobilization of ferromagnetic particles enables non-contact manipulation and efficient magnetic separation for process intensification in biotechnological applications. In this study, *Aspergillus oryzae* was cultivated in the presence of magnetite or a magnetite-activated carbon composite to promote particle incorporation during pellet growth. Morphological analysis based on image processing revealed a concentration-dependent increase in pellet size, accompanied by internal particle agglomeration. Additionally, magnetic labelling was achieved post-cultivation by incubating mature pellets with suspended particles, allowing for flexible integration into existing processes. Both approaches yielded magnetically responsive fungal biocomposites that could be readily separated using external magnetic fields, highlighting their potential for biomass retention, recovery and process intensification.

1. Introduction

Fungi are widely adopted in industrial biotechnology for the production of various valuables including proteins and small-molecule metabolites [1]. Filamentous fungi grow as branching hyphae, forming interconnected mycelial networks and aggregating into macroscopic dense structures known as pellets [2]. Pellet morphology varies depending on species as well as on cultivation conditions and correlates with production performance. For instance, compact pellets are associated with higher citric acid productivities in *Aspergillus niger* [3].

Fungal morphology is modulated by abiotic factors such as the addition of water-insoluble particles. Hence, process intensification by addition of small particles to enhance performance in filamentous cultivation is known as microparticle-enhanced cultivation (MPEC) [4–6]. *A. niger* incubated with $TiSiO_4$ particles grows in core-shell pellets, enhancing mass transfer by decreasing pellet size and density and increasing the titers of fructofuranosidase and glucoamylase by 3.7-fold and 9.5-fold, respectively [7]. Addition of talcum to cultures of *Aspergillus sojae* reduces pellet diameter and enhances activity of polygalacturonase up to a 9-fold increase [8].

MPEC provides an opportunity for functionalization of fungal biomass, as the incorporated particles impart their specific properties to the biomass. One such feature is ferromagnetism, imparted to activated carbon through microwave-assisted synthesis with $Fe(OH)_2$ by Pfitzer et al. [9]. The same authors demonstrated the biomass-adsorbing properties of the resulting composite of magnetite and activated carbon particles ($P_{MAG/AC}$) with cells of *Shewanella oneidensis*. This study is based on similar principles, immobilizing $P_{MAG/AC}$ in pellets of the mold *Aspergillus oryzae* to functionalize biomass and exploit the MPEC effect during fungal growth.

While magnetic particle immobilization in microbial systems has been explored previously, including applications such as nitrate removal using denitrifying bacteria immobilized within magnetically functionalized mycelium pellets and environmental remediation with fungus-based magnetic nanobiocomposites, magnetic strategies have also been applied for increased current production in bioelectrochemical systems [10–12]. In contrast to previous studies, the present work investigates the incorporation of $P_{MAG/AC}$ composite particles into pellets of the industrially relevant filamentous fungus *Aspergillus oryzae* under submerged cultivation conditions. $P_{MAG/AC}$ particles combine the high surface area and adsorptive properties of activated carbon with the magnetic functionality of magnetite, enabling a dual-purpose material for fungal biomass functionalization. To the best of our knowledge, this represents the first demonstration of magnetic particle immobilization

* Corresponding author.
E-mail addresses: lukas.hartmann@kit.edu (L. Hartmann), marina.schreidl@student.kit.edu (M. Schreidl), pyschik@posteo.de (M. Pyschik), markus.stoeckl@dechema.de (M. Stöckl), dirk.holtmann@kit.edu (D. Holtmann).

https://doi.org/10.1016/j.cep.2026.110750
Received 5 September 2025; Received in revised form 20 December 2025; Accepted 13 February 2026
Available online 14 February 2026
0255-2701/© 2026 The Author(s). Published by Elsevier B.V. This is an open access article under the CC BY license (http://creativecommons.org/licenses/by/4.0/).

in an industrially relevant *Aspergillus species*. Beyond incorporation, this work examines the impact of particles on pellet morphology and structural heterogeneity. The study provides qualitative microscopic analysis of particle-hypha interactions and compares the incorporation of distinct particle types. Overall, this work advances the concept of magnetic particle-enabled cultivation by extending it toward functional magnetization of industrially relevant fungal biomass and highlighting its potential for process intensification in biomass handling.

2. Methods

2.1. Microorganism and media

Aspergillus oryzae DSM 1863 was obtained from the DSMZ strain collection (Deutsche Sammlung von Mikroorganismen und Zellkulturen GmbH, Braunschweig, Germany). Media were prepared using demineralized water. Conidia propagation followed a procedure similar to that described by Kövilein et al. [13], using *Aspergillus* minimal medium containing 15 g L^{-1} glucose monohydrate, 6 g L^{-1} $NaNO_3$, 22.37 g L^{-1} KCl, 0.52 g L^{-1} $MgSO_4{\cdot}7H_2O$, 1.52 g L^{-1} KH_2PO_4 and 15 g L^{-1} agar [14,15]. Additionally, 2 mL L^{-1} of Hutner's Trace Elements (HTE) was added. The pH was set to 6.5 with NaOH, and the medium was sterilized by autoclaving at 121°C for 20 minutes. The trace element solution included 5 g L^{-1} $FeSO_4{\cdot}7H_2O$, 50 g L^{-1} Na_2EDTA, 22 g L^{-1} $ZnSO_4{\cdot}7H_2O$, 11 g L^{-1} H_3BO_3, 5 g L^{-1} $MnCl_2{\cdot}4H_2O$, 1.6 g L^{-1} $CoCl_2{\cdot}6H_2O$, 1.6 g L^{-1} $CuSO_4{\cdot}5H_2O$ and 1.1 g L^{-1} $(NH_4)_6Mo_7O_{24}{\cdot}4H_2O$ at pH 6.5 and was sterilized via 0.2 µm filtration [16]. After incubation for 6 d at 30°C, conidia were collected in 50% (v/v) glycerol, filtered through Miracloth (Merck KGaA, Darmstadt, Germany), quantified and stored in aliquots at -20°C.

The medium for submerged growth of *A. oryzae* in shake flasks (SF) for particle immobilization was prepared following the protocol described by Kövilein et al. [17]. The composition contained 40 g L^{-1} glucose monohydrate, 4 g L^{-1} $(NH_4)_2SO_4$, 0.75 g L^{-1} KH_2PO_4, 0.98 g L^{-1} K_2HPO_4, 0.1 g L^{-1} $MgSO_4{\cdot}7H_2O$, 0.1 g L^{-1} $CaCl_2{\cdot}2H_2O$, 5 mg L^{-1} NaCl and 5 mg L^{-1} $FeSO_4{\cdot}7H_2O$. All components except HTE were autoclaved together. Before inoculation, 2 mL L^{-1} of HTE was added to the medium and non-sterile particles were aseptically added to sterile SF. After cultivation, the SF were visually inspected for clarity of the medium, growth of contaminants was not observed.

2.2. Particle synthesis and properties

$P_{MAG/AC}$ fabrication was conducted via alkaline iron precipitation and microwave-assisted synthesis and followed the protocol described by Pfitzer et al. [9]. Briefly, $P_{MAG/AC}$ were produced by microwave irradiation of $FeSO_4{\cdot}7H_2O$ in an alkaline reaction medium in the presence of activated carbon (AC) particles (Alcarbon DC 1000/80 × 325, Donau Carbon, Frankfurt am Main, Germany). 10 g $FeSO_4{\cdot}7H_2O$ were dissolved in 80 mL distilled water and 1 g of AC was added. Subsequently, NaOH was added to adjust the pH to approximately 12. The dispersion was placed into a microwave (Etos.lab microwave system, MLS GmbH, Leutkirch, Germany) and irradiated at 1600 W in 15 pulses of 100 s, with subsequent cooling phases below 60°C after each pulse. Obtained $P_{MAG/AC}$ particles were harvested using a permanent neodymium magnet and cleaned by multiple washing steps with demineralized water and ethanol.

In order to approximate comparable particle volumes during cultivation, the tapped density of each particle type, as shown in Table 1, was determined by filling a defined volume with the respective powder, tapping, and weighing. For the $P_{MAG/AC}$ composite particles, the tapped density was approximated using the precursor material Alcarbon DC 1000/80 × 325.

2.3. Immobilization of particles during fungal growth

100 mL of $P_{MAG/AC}$ or magnetite containing medium was inoculated with 2 × 10^5 conidia mL^{-1} and incubated in 500 mL baffled SF at 100 rpm, an orbital diameter of 25 mm and 30°C for 24 h. The concentration of magnetite was increased 4-fold based on the ratio of tapped densities of magnetite and $P_{MAG/AC}$, providing similar volumes of submerged particles. Cultivations were performed in biological triplicates. After cultivation, the broth was sieved through a 0.5 mm mesh size and the filtrate was measured for pH (Lab845, Xylem Analytics Germany Sales GmbH & Co. KG). The description of pH measurements can be found in Supplement 1. Immobilization of particles in the retentate pellets was investigated after washing with demineralized water, visualization by scanning with 2400 dpi (Perfection V600 Photo, Epson Deutschland GmbH, Düsseldorf, Germany) and performing microscopic analysis (Eclipse E200 LED, Nikon Instruments Europe B.V., Amstelveen, Netherlands).

Table 1
Particle size and tapped density of materials used in this study. Size ranges refer to manufacturer specifications. $P_{MAG/AC}$ density was not determined.

Particles	Size [µm]	Tapped density [g mL^{-1}]	Reference
Alcarbon DC 1000	45 - 180	0.58	Donau Carbon GmbH, Frankfurt a. Main, Germany
$P_{MAG/AC}$	100 - 300	-	[9]
Magnetite (extra fine)	d_{50}: 2.6	2.36	Kremer Pigmente GmbH & Co. KG, Aichstetten, Germany

2.4. Morphological analysis of fungal pellets

Morphological image analysis was conducted using a MATLAB R2024b script (The MathWorks, Natick, Massachusetts, United States). Flatbed scanner images were downscaled, converted to grayscale and pre-processed to exclude edge regions. Particle segmentation was based on adaptive thresholding applied to the grayscale image, generating a foreground mask that distinguishes darker structures from the background. Morphological operations were applied to suppress noise and refine object boundaries. Object detection was performed by identifying connected regions within the segmented mask. Detected objects were filtered based on an aspect ratio threshold of 3, a maximum object length of 1000 pixels, a minimum area equivalent to 0.01 mm^2, an exclusion of particles located within fixed image margins and a removal of objects with grayscale intensity values above the 80th percentile of all detected regions in the image. This intensity-based filtering step was applied to exclude artifacts or reflections that are considerably brighter than the majority of particles and are unlikely to represent relevant pellet structures. The script can be found in Supplement 2.

2.5. Displaying magnetized biomass

In order to verify the ferromagnetization of fungal pellets, a high-strength Ni-coated permanent magnet of grade N40 with dimensions of 50.8 × 50.8 × 25.4 mm was positioned adjacent to a water suspension of fungal pellets containing ferromagnetic particles. The movement and aggregation of the indirect ferromagnetized pellets were documented through digital imaging. Images were taken using a Samsung Galaxy M30s (Samsung Electronics Co., Ltd., Suwon, South Korea) equipped with a 48-megapixel main camera. Photos were captured in automatic mode using the camera application version 11.0.15.99 without any manual adjustments.

2.6. Immobilization of particles by short-term incubation

0.1 g *A. oryzae* pellets were incubated in 500 µL of 4 g L^{-1} $P_{MAG/AC}$ and 28 g L^{-1} magnetite suspensions at 30°C, 1000 rpm and an orbital diameter of 3 mm for 30 min. Immobilization was confirmed via

microscopic analysis.

3. Results and discussion

3.1. Immobilization of particles during fungal growth

Morphology of fungal biomass at varying concentrations of $P_{MAG/AC}$ and magnetite is illustrated in Fig. 1. Particle concentrations were selected to approximate equivalent total particle volumes across both materials, accounting for differing densities. At low concentrations, pellets appeared uniform with few visible embedded particles. As concentrations rose, pellets tended to exhibit more irregular outlines and a visibly higher number of incorporated particles. At the highest concentrations, the pellets appeared more heterogeneous, with dense particle inclusion suggesting altered pellet architecture. These visual trends are quantitatively supported by image-based morphological analysis of the 2D projected pellet area. In both series, median pellet size increased with rising particle concentration, particularly at 1.6 g L^{-1} for $P_{MAG/AC}$ and 25.6 g L^{-1} for magnetite, respectively. Notably, magnetite supplementation at 25.6 g L^{-1} resulted in a strong broadening of the pellet size distribution, indicating heterogeneous pellet growth.

Morphological diversity of *A. oryzae* pellets containing immobilized particles is shown in Fig. 2. Particles appeared concentrated in the pellet core, often forming dense, dark central regions. Radial hyphal outgrowth remained visible in many cases, but was frequently altered in symmetry and density, suggesting that particle inclusion impacted pellet architecture. Several images show disrupted or asymmetric morphologies, indicative of heterogeneous particle distribution and potentially pellet restructuring. At the highest particle concentrations, pellet formation was severely impaired, and large, compact agglomerates of particles in the core regions are observed.

When particles are present during the initial growth phase, fungal hyphae may grow around them, resulting in structural incorporation. In this scenario, we hypothesize that particle clusters act as nucleation points around which hyphae extend and enclose the material. This hypothesis is supported by microscopy images showing radial hyphal structures seemingly emerging from particle aggregates, as shown in Fig. 2. Similar overgrowth has been previously described for *A. niger* with $TiSiO_4$ particles [7], although static images alone cannot prove active encapsulation.

Adhesion of ferromagnetic particles to fungal hyphae is demonstrated in Fig. 3. The particles appeared as dark, high-contrast structures tightly associated with the hyphal surfaces. In several regions, they formed continuous lines or localized clusters. This observation confirms the particle-hypha interaction at the microscale and supports the macroscopic findings shown in Fig. 2.

Magnetic response of fungal biomass associated with ferromagnetic particles is shown in Fig. 4. The strength of the magnetic field increases with decreasing distance to the magnet, following a nonlinear gradient approximately proportional to r^{-3} for a dipole field [18]. This field gradient generates a magnetic force acting on magnetite-containing fungal pellets, promoting rapid and directed aggregation. Pellets

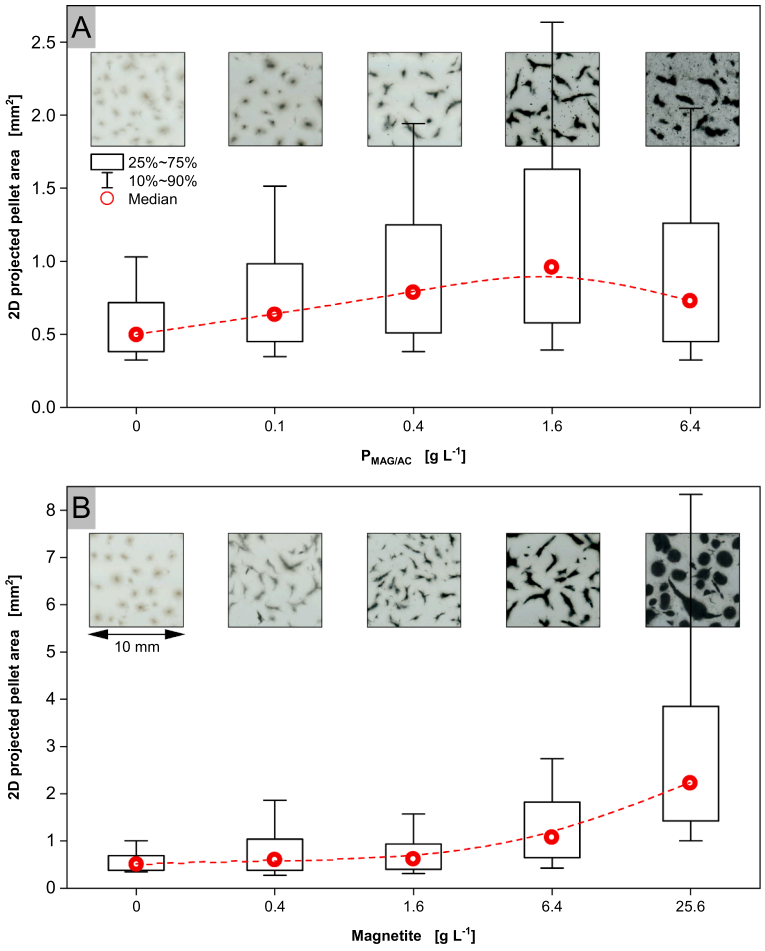

Fig. 1. 2D projected pellet area and scans of *Aspergillus oryzae* DSM 1863 pellets after 24 h growth with ferromagnetic particles. Depicted and analyzed pellets originate from one SF per particle concentration. Images illustrate exemplary groups of pellets. Area analysis considered 500 to 2200 pellets per image. Cultivations were performed with X_0 of 2 × 10^5 conidia mL^{-1}, 36 g L^{-1} glucose, V_0 of 100 mL, 30°C, 100 rpm at an orbital diameter of 25 mm. pH values of cultivations are contained in Supplement 1.

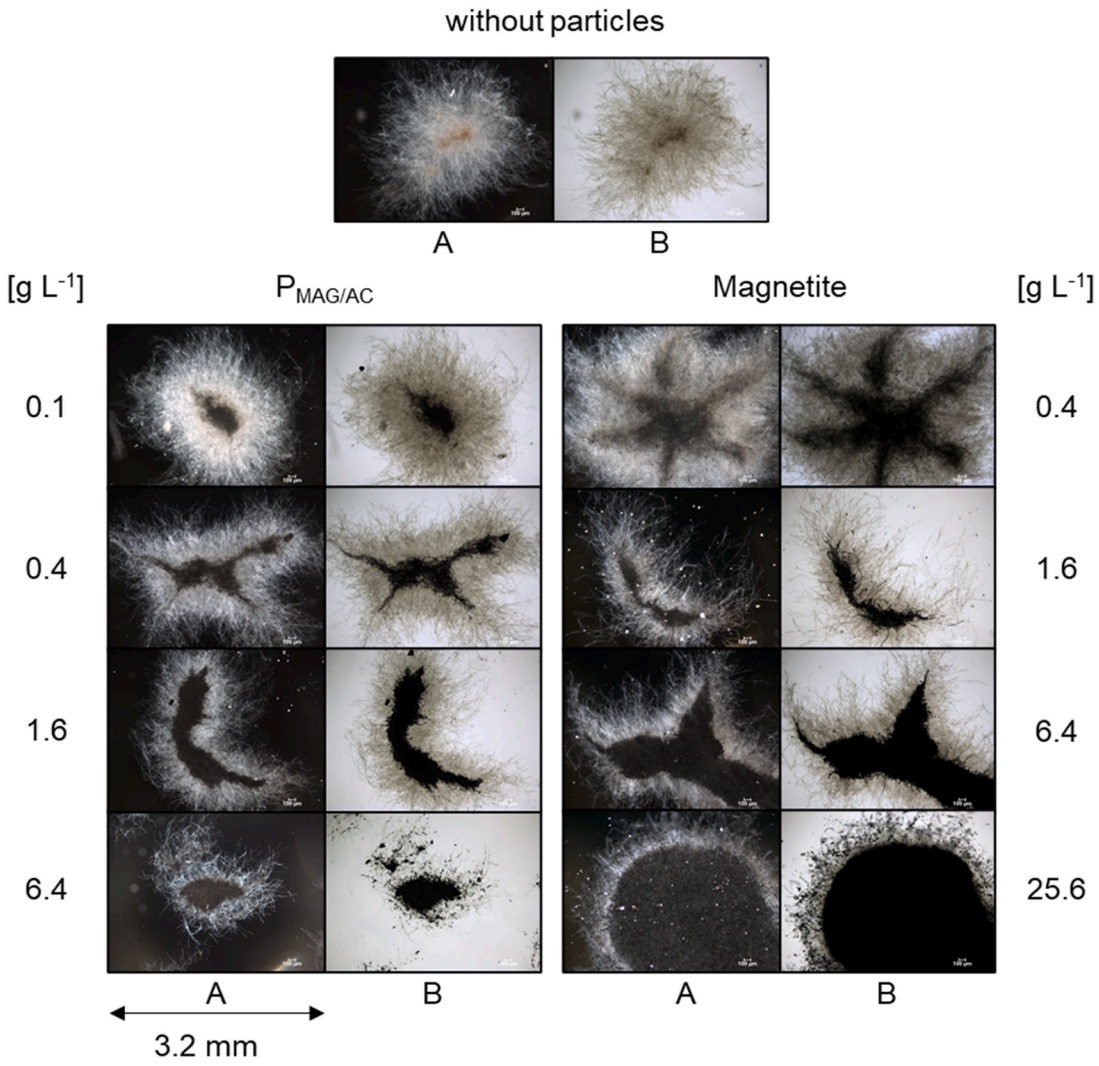

Fig. 2. Microscopic analysis of *Aspergillus oryzae* DSM 1863 pellets after 24 h growth with ferromagnetic particles. For images in A, brightfield microscopy was performed under reduced illumination intensity; images in B were acquired under standard brightfield conditions. Samples were taken after 24 h of cultivation. Cultivations were performed with X_0 of 2 × 10^5 conidia mL^{-1}, 36 g L^{-1} glucose, V_0 of 100 mL, 30°C, 100 rpm at an orbital diameter of 25 mm.

grown in 6.4 g L^{-1} magnetite showed the strongest response, forming dense layers even at larger distances. In contrast, pellets grown in 1.6 g L^{-1} magnetite and 1.6 g L^{-1} $P_{MAG/AC}$ exhibited moderate attraction, indicating lower magnetic susceptibility at larger distances.

The observed magnetic attraction demonstrates that particle-infused fungal biomass can be effectively manipulated under an external magnetic field, enabling potential applications such as biomass separation from liquid media for cell recovery, for example through filtration retaining cells via a magnetic field [19]. For readers seeking a comprehensive introduction to the physical principles underlying magnetic separation and the characteristics of magnetic particles in biological systems, several recent reviews provide detailed discussions of magnetic particle synthesis, magnetic forces and bioseparation methodologies [20–22]. Moreover, magnetic fungal pellets could be immobilized using external magnets in continuous cultivation by supporting natural surface adhesion through magnetic attraction [23]. Similar to magnetic levitation of single cells by Durmus et al., external magnetic fields could be used to levitate particle-infused fungal biomass, allowing for precise spatial positioning and research in the absence of wall-induced distortions [24]. Magnetic immobilization could also allow biomass to remain suspended in solvents with mismatched polarity and density. Similar to the adsorption of *S. oneidensis* by Pfitzer et al., other microorganisms could be adsorbed onto activated carbon, facilitating interactions within the fungal pellets and fostering the development of novel microbial ecosystems [9].

3.2. Immobilization of particles by short-term incubation

Fungal pellets grown after 24 h of cultivation without particles were incubated with ferromagnetic particles for 30 min. Microscopic analysis in Fig. 5 revealed that the mycelium retained these particles within the pellet structure. Notably, particle accumulation followed a concentric pattern, with the highest density observed around the pellet core. The core region remained brighter in phase contrast images, indicating a comparatively lower particle content in this area.

These observations demonstrate that particle incorporation can occur after pellet formation, allowing magnetic functionalization of the biomass without interfering with pellet growth or morphology. Such an approach is particularly advantageous, as high concentrations of magnetite may negatively affect fungal growth. Inhibitory effects of magnetite have been reported across a wide range of fungal genera, including *Trichothecium, Cladosporium, Penicillium, Alternaria*, and *Aspergillus* [25,26]. Similarly, high amounts of activated carbon could potentially impair growth due to its adsorptive properties, sequestering nutrients from the medium [27].

The particles were not removed by washing and withstood rapid

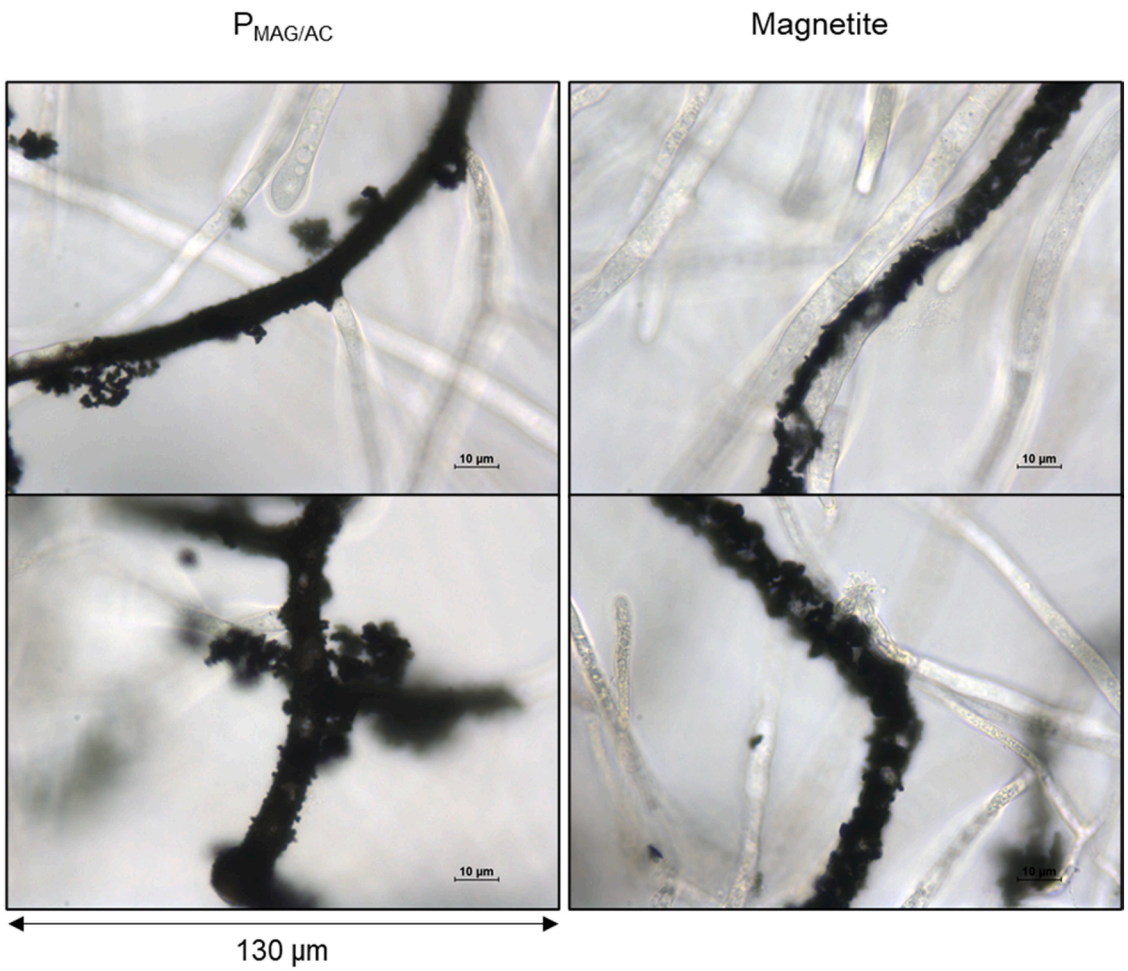

Fig. 3. Microscopic analysis of *Aspergillus oryzae* DSM 1863 pellets after 24 h growth with ferromagnetic particles. Images were taken with phase contrast microscopy.

shaking, implying strong mechanical fixation or physicochemical retention. Based on previously reported properties of *Aspergillus* conidia and hyphae, and the known surface characteristics of $P_{MAG/AC}$ and magnetite, several mechanisms are proposed as plausible explanations for this behavior: Hyphal surfaces are not smooth; local roughness, vesicles or extracellular structures may enhance mechanical adhesion through microscale interlocking with porous or irregular particle surfaces [28]. Similarly, previous work has shown that the topography of the surface to which spores attach strongly influences adhesion [29]. In addition, a viscoelastic matrix composed of polysaccharides or glycoproteins may act as biological glue, capturing particles more effectively [30–32]. In particular, galactosaminogalactan, a functional component of this extracellular matrix, can remain associated with the hyphal surface and influence adhesion. Moreover, studies have provided evidence that negatively charged carbohydrates on the surface of *Aspergillus* conidia contribute to adhesion via electrostatic interactions [33]. Evidence for this mechanism comes from the negative ζ-potential of *Aspergillus* conidia across the pH range from 2 to 6, in contrast to the positive surface potential of magnetite below pH 5 [34,35]. Given the pH drop to around 2 during fungal growth, it is plausible that *Aspergillus* conidia electrostatically adhere to the surfaces of $P_{MAG/AC}$ or magnetite particles under such conditions. In contrast to particle incorporation during pellet growth, microscopy of experiments where pre-grown pellets were incubated with particles revealed rapid penetration and retention of particles primarily within the peripheral regions. This indicates a mechanism based on physical entrapment, likely driven by capillary forces and the porous architecture of the mature mycelial network [36].

4. Conclusion

This study demonstrates the successful incorporation of functional magnetic $P_{MAG/AC}$ particles into *A. oryzae* pellets during and after fungal growth. Morphological analysis based on image processing revealed a concentration-dependent increase in pellet size accompanied by internal particle agglomeration. The method of particle incorporation, either during pellet growth or through short-term post-cultivation incubation, strongly influenced particle distribution within fungal pellets, indicating that structural incorporation and physical entrapment contribute to particle immobilization. These findings provide a foundation for the development of magnetically addressable fungal biocatalysts and open new avenues for process intensification, optimizing biomass handling and downstream processing.

Declaration of generative AI and AI-assisted technologies in the manuscript preparation process

During the preparation of this work the authors used Microsoft Copilot (GPT-4, Microsoft Corporation, Redmond, Washington, United States) in order to improve language clarity and assist with code development. After using this tool, the authors reviewed and edited the content as needed and take full responsibility for the content of the published article.

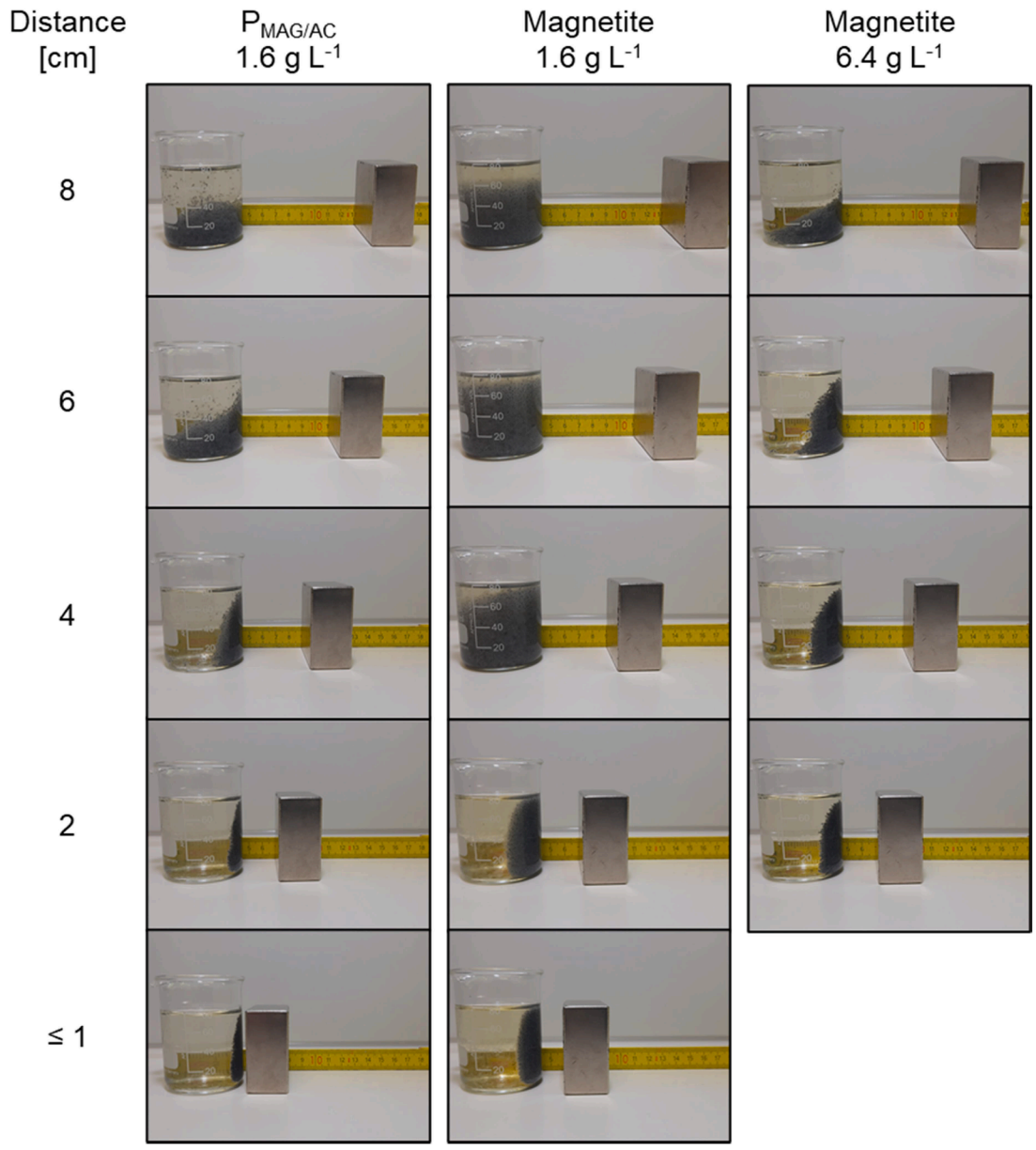

Fig. 4. Magnetic attraction of *Aspergillus oryzae* DSM 1863 pellets with immobilized $P_{MAG/AC}$ and magnetite in demineralized water. Pellets originate from fungal growth in medium suspensions containing 1.6 g L^{-1} $P_{MAG/AC}$ and 1.6 g L^{-1} or 6.4 g L^{-1} magnetite, respectively. Images were taken after pellet movement had ceased. Image at $\leq$ 1 cm distance of pellets from cultivation with 6.4 g L^{-1} magnetite was omitted due to intense attraction between the glass vessel and the magnet.

Funding statement

This research received no external funding.

Ethics approval statement

Not applicable.

Patient consent statement

Not applicable.

Permission to reproduce material from other sources

Not applicable.

Clinical trial registration

Not applicable.

CRediT authorship contribution statement

Lukas Hartmann: Writing – review & editing, Writing – original draft, Visualization, Software, Methodology, Investigation, Formal analysis, Conceptualization. **Marina Schreidl:** Methodology, Investigation, Conceptualization. **Markus Pyschik:** Investigation. **Markus Stöckl:** Writing – review & editing, Resources. **Dirk Holtmann:** Writing – review & editing, Supervision, Resources, Conceptualization.

Declaration of competing interest

The authors declare no competing interests.

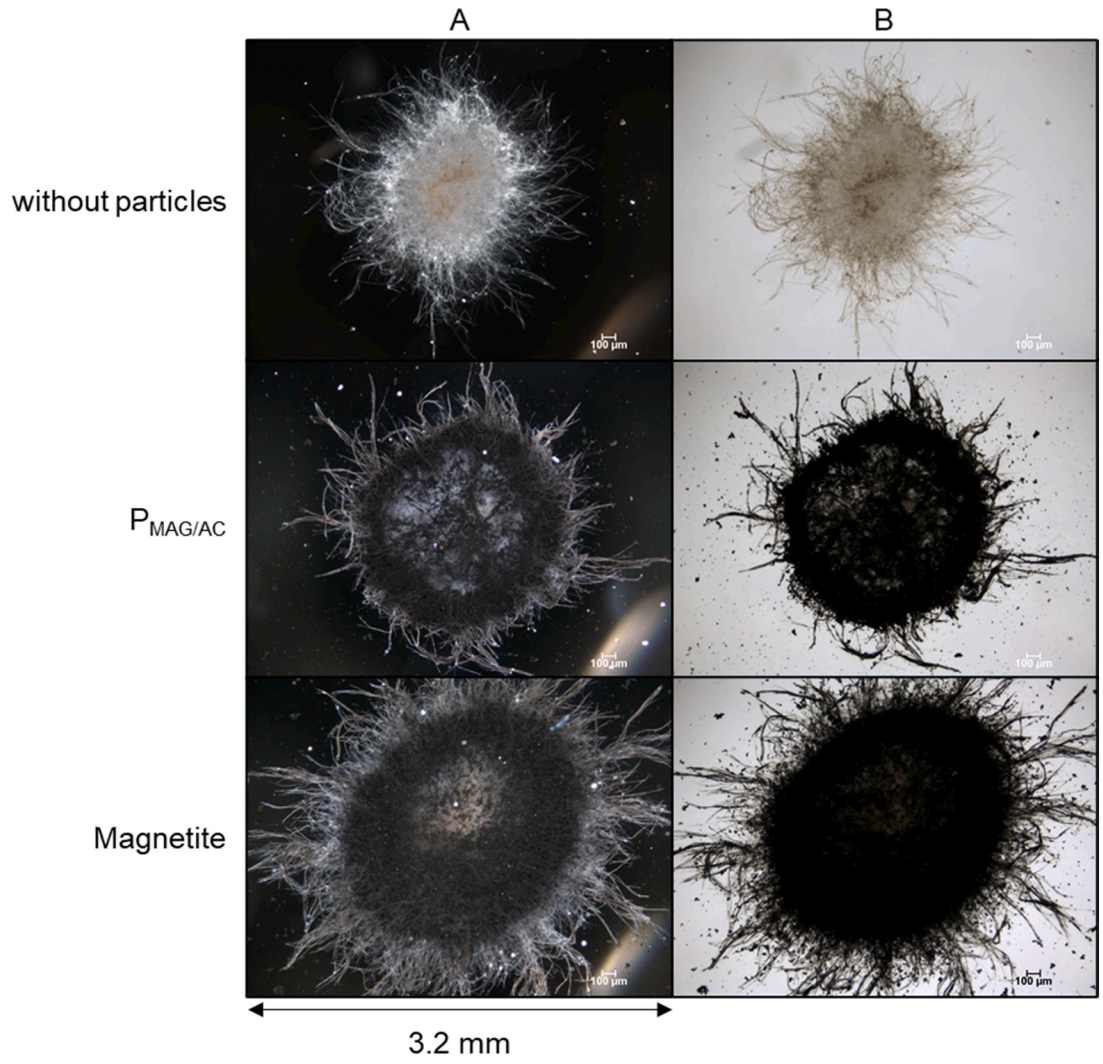

Fig. 5. Microscopic analysis of *Aspergillus oryzae* DSM 1863 pellets after 30 min incubation with ferromagnetic particles. For images in A, brightfield microscopy was performed under reduced illumination intensity; images in B were acquired under standard brightfield conditions. 500 µL of 4 g L^{-1} $P_{MAG/AC}$ and 28 g L^{-1} magnetite suspensions in demineralized water were incubated with 0.1 g *A. oryzae* pellets at 30°C, 1000 rpm and an orbital diameter of 3 mm for 30 min.

Supplementary materials

Supplementary material associated with this article can be found, in the online version, at doi:10.1016/j.cep.2026.110750.

Data availability

Data will be made available on request.

References

[1] A.E. Posch, C. Herwig, O. Spadiut, Science-based bioprocess design for filamentous fungi, Trends Biotechnol. 31 (1) (2013) 37–44, https://doi.org/10.1016/j.tibtech.2012.10.008.

[2] Z. Lu, Z. Chen, Y. Liu, X. Hua, C. Gao, J. Liu, Morphological Engineering of Filamentous Fungi: Research Progress and Perspectives, J. Microbiol. Biotechnol. 34 (6) (2024) 1197–1205, https://doi.org/10.4014/jmb.2402.02007.

[3] X. Yin, H.D. Shin, J. Li, G. Du, L. Liu, J. Chen, Comparative genomics and transcriptome analysis of *Aspergillus niger* and metabolic engineering for citrate production, Sci. Rep. 7 (2017) 41040, https://doi.org/10.1038/srep41040.

[4] E. Karahalil, H.B. Coban, I. Turhan, A current approach to the control of filamentous fungal growth in media: microparticle enhanced cultivation technique, Crit. Rev. Biotechnol. 39 (2) (2019) 192–201, https://doi.org/10.1080/07388551.2018.1531821.

[5] J. Walisko, F. Vernen, K. Pommerehne, G. Richter, J. Terfehr, D. Kaden, L. Dähne, D. Holtmann, R. Krull, Particle-based production of antibiotic rebeccamycin with *Lechevalieria aerocolonigenes*, Process Biochem. 53 (2017) 1–9, https://doi.org/10.1016/j.procbio.2016.11.017.

[6] M.M. Etschmann, I. Huth, R. Walisko, J. Schuster, R. Krull, D. Holtmann, C. Wittmann, J. Schrader, Improving 2-phenylethanol and 6-pentyl-alpha-pyrone production with fungi by microparticle-enhanced cultivation (MPEC), Yeast 32 (1) (2015) 145–157, https://doi.org/10.1002/yea.3022.

[7] H. Driouch, R. Hänsch, T. Wucherpfennig, R. Krull, C. Wittmann, Improved enzyme production by bio-pellets of *Aspergillus niger*: targeted morphology engineering using titanate microparticles, Biotechnol. Bioeng. 109 (2) (2012) 462–471, https://doi.org/10.1002/bit.23313.

[8] M. Germec, E. Karahalil, E. Yatmaz, C. Tari, I. Turhan, Effect of process parameters and microparticle addition on polygalacturonase activity and fungal morphology of *Aspergillus sojae*, Biomass Convers. Biorefin. 12 (11) (2021) 5329–5344, https://doi.org/10.1007/s13399-021-02096-3.

[9] M. Pfitzer, F. Mayer, K.-M. Mangold, D. Holtmann, M. Stöckl, Straightforward synthesis of magnetized activated carbon particles, Nano-Struct. Nano-Objects 30 (2022), https://doi.org/10.1016/j.nanoso.2022.100875.

[10] Y. Sun, A. Ali, Z. Zheng, J. Su, S. Zhang, Y. Min, Y. Liu, Denitrifying bacteria immobilized magnetic mycelium pellets bioreactor: A new technology for efficient removal of nitrate at a low carbon-to-nitrogen ratio, Bioresour. Technol. 347 (2022) 126369, https://doi.org/10.1016/j.biortech.2021.126369.

[11] T.d.O. Chaves, R.D. Bini, V.A.d. Oliveira Junior, A.D. Polli, A. Garcia, G.S. Dias, I.A. d. Santos, P. Nunes de Oliveira, J.A. Pamphile, L.F. Cotica, Fungus-based magnetic nanobiocomposites for environmental remediation, Magnetochemistry 8 (11) (2022), https://doi.org/10.3390/magnetochemistry8110139.

[12] T. Arinda, L.A. Philipp, D. Rehnlund, M. Edel, J. Chodorski, M. Stöckl, D. Holtmann, R. Ulber, J. Gescher, K. Sturm-Richter, Addition of Riboflavin-coupled magnetic beads increases current production in bioelectrochemical systems via the increased formation of anode-biofilms, Front. Microbiol. 10 (2019) 126, https://doi.org/10.3389/fmicb.2019.00126.

[13] A. Kövilein, J. Umpfenbach, K. Ochsenreither, Acetate as substrate for L-malic acid production with *Aspergillus oryzae* DSM 1863, Biotechnol. Biofuels. 14 (1) (2021) 48, https://doi.org/10.1186/s13068-021-01901-5.
[14] R.W. Barratt, G.B. Johnson, W.N. Ogata, Wild-type and mutant stocks of *Aspergillus nidulans*, Genetics 52 (1) (1965) 233–246, https://doi.org/10.1093/genetics/52.1.233.
[15] M.H. Song, J.-y. Nah, Y.S. Han, D.M. Han, K.-S. Chae, Promotion of conidial head formation in *Aspergillus oryzae* by a salt, Biotechnol. Lett. 23 (9) (2001) 689–691, https://doi.org/10.1023/a:1010308601469.
[16] T.W. Hill, E. Kafer, Improved protocols for *Aspergillus* minimal medium: trace element and minimal medium salt stock solutions, Fungal Genet. Rep. 48 (1) (2001) 20–21, https://doi.org/10.4148/1941-4765.1173.
[17] A. Kövilein, V. Aschmann, S. Hohmann, K. Ochsenreither, Immobilization of *Aspergillus oryzae* DSM 1863 for L-Malic acid production, Fermentation 8 (1) (2022) 26, https://doi.org/10.3390/fermentation8010026.
[18] S.V. Starchenko, C.A. Jones, Typical velocities and magnetic field strengths in planetary interiors, Icarus 157 (2) (2002) 426–435, https://doi.org/10.1006/icar.2002.6842.
[19] J.H.P. Watson, Magnetic filtration, J. Appl. Phys. 44 (9) (1973) 4209–4213, https://doi.org/10.1063/1.1662920.
[20] M. Frenea-Robin, J. Marchalot, Basic principles and recent advances in magnetic cell separation, Magnetochemistry 8 (1) (2022), https://doi.org/10.3390/magnetochemistry8010011.
[21] B.D. Plouffe, S.K. Murthy, L.H. Lewis, Fundamentals and application of magnetic particles in cell isolation and enrichment: a review, Rep. Prog. Phys. 78 (1) (2015) 016601, https://doi.org/10.1088/0034-4885/78/1/016601.
[22] L. Borlido, A.M. Azevedo, A.C. Roque, M.R. Aires-Barros, Magnetic separations in biotechnology, Biotechnol. Adv. 31 (8) (2013) 1374–1385, https://doi.org/10.1016/j.biotechadv.2013.05.009.
[23] M. Ogawa, L.F. Bisson, T. Garcia-Martinez, J.C. Mauricio, J. Moreno-Garcia, New insights on yeast and filamentous fungus adhesion in a natural co-immobilization system: proposed advances and applications in wine industry, Appl. Microbiol. Biotechnol. 103 (12) (2019) 4723–4731, https://doi.org/10.1007/s00253-019-09870-4.
[24] N.G. Durmus, H.C. Tekin, S. Guven, K. Sridhar, A. Arslan Yildiz, G. Calibasi, I. Ghiran, R.W. Davis, L.M. Steinmetz, U. Demirci, Magnetic levitation of single cells, Proc. Natl. Acad. Sci. U S. A 112 (28) (2015) E3661–E3668, https://doi.org/10.1073/pnas.1509250112.
[25] S. Parveen, A.H. Wani, M.A. Shah, H.S. Devi, M.Y. Bhat, J.A. Koka, Preparation, characterization and antifungal activity of iron oxide nanoparticles, Microb. Pathog. 115 (2018) 287–292, https://doi.org/10.1016/j.micpath.2017.12.068.
[26] K. Vijayalakshmi, T. Swaramanjari, M. Shanmugavel, A. Gnanamani, Green-synthesized metal and metal oxide nanoparticles as emerging antifungal agents: current advances, mechanisms, and future perspectives, Discov. Biotechnol. 2 (1) (2025), https://doi.org/10.1007/s44340-025-00024-z.
[27] S.M. Praveena, U. Rashid, S. Abdul Rashid, Optimization of nutrients removal from synthetic greywater by low-cost activated carbon: application of Taguchi method and response surface methodology, Toxin Rev. 41 (2) (2021) 506–515, https://doi.org/10.1080/15569543.2021.1903037.
[28] H.U. Lee, J.B. Park, H. Lee, K.S. Chae, D.M. Han, K.Y. Jahng, Predicting the chemical composition and structure of *Aspergillus nidulans* hyphal wall surface by atomic force microscopy, J. Microbiol. 48 (2) (2010) 243–248, https://doi.org/10.1007/s12275-010-8094-4.
[29] K.A. Whitehead, C.M. Liauw, S. Lynch, M. El Mohtadi, M. Amin, A. Preuss, T. Deisenroth, J. Verran, Diverse surface properties reveal that substratum roughness affects fungal spore binding, iScience 24 (4) (2021) 102333, https://doi.org/10.1016/j.isci.2021.102333.
[30] M.J. Lee, D.C. Sheppard, Recent advances in the understanding of the *Aspergillus fumigatus* cell wall, J. Microbiol. 54 (3) (2016) 232–242, https://doi.org/10.1007/s12275-016-6045-4.
[31] D.C. Sheppard, P.L. Howell, Biofilm exopolysaccharides of pathogenic fungi: lessons from bacteria, J. Biol. Chem. 291 (24) (2016) 12529–12537, https://doi.org/10.1074/jbc.R116.720995.
[32] A. Beauvais, C. Schmidt, S. Guadagnini, P. Roux, E. Perret, C. Henry, S. Paris, A. Mallet, M.C. Prevost, J.P. Latge, An extracellular matrix glues together the aerial-grown hyphae of *Aspergillus fumigatus*, Cell Microbiol. 9 (6) (2007) 1588–1600, https://doi.org/10.1111/j.1462-5822.2007.00895.x.
[33] J.A. Wasylnka, M.M. Moore, Adhesion of *Aspergillus* species to extracellular matrix proteins: evidence for involvement of negatively charged carbohydrates on the conidial surface, Infect. Immun. 68 (6) (2000) 3377–3384, https://doi.org/10.1128/IAI.68.6.3377-3384.2000.
[34] S.M. Vidojkovic, M.P. Rakin, Surface properties of magnetite in high temperature aqueous electrolyte solutions: a review, Adv. Colloid. Interface Sci. 245 (2017) 108–129, https://doi.org/10.1016/j.cis.2016.08.008.
[35] A. Wargenau, A. Fleissner, C.J. Bolten, M. Rohde, I. Kampen, A. Kwade, On the origin of the electrostatic surface potential of *Aspergillus niger* spores in acidic environments, Res. Microbiol. 162 (10) (2011) 1011–1017, https://doi.org/10.1016/j.resmic.2011.07.006.
[36] Sun, M. Tajvidi, C. Howell, C.G Hunt, Insight into mycelium-lignocellulosic biocomposites: essential factors and properties, Compos. A-Appl. Sci. Manuf. 161 (2022), https://doi.org/10.1016/j.compositesa.2022.107125.